GMR
The Original

PHYSICOCHEMICAL CHARACTERIZATION AND ANTI-INFLAMMATORY POTENTIAL OF BIOCOMPATIBLE STARCH/PVA/ CuO ELECTROSPUN NANOSCAFFOLDS FROM *Sargassum muticum* (BROWN MARINE MACROALGAE) EXTRACT

Sheetal Raman Murugaiyan[1], Sanjay Surya R[2], Anand KH[3], Nishandhini Marimuthu[4]*, Kamaraj Raju[5]*

[1]Saveetha Medical College & Hospital (SMCH), Saveetha Institute of Medical and Technical Sciences (SIMATS), Thandalam, Chennai, Tamil Nadu 602105, India. rmsheetal157@gmail.com
2Department of Anaesthesiology, Saveetha Medical College and Hospital, Saveetha Institute of Medical And Technical Sciences (SIMATS), Thandalam, Chennai-602105, Tamil Nadu, India. Email: sanjaysurya1997@gmail.com; ORCID: https://orcid.org/0009-0005-9187-8496.
[3]Department of ENT, Saveetha Medical College and Hospital, Saveetha Institute of Medical And Technical Sciences (SIMATS), Thandalam, Chennai-602105, Tamil Nadu, India. Email: anandkh91@gmail.com. ORCID: https://orcid.org/0000-0001-8496-5675.
[4]Department of Bioinformatics, School of Life Sciences, Vels Institute of Science Technology and Advanced Studies, Pallavaram,Chennai-600117, Tamil Nadu, India. Email: enishay30@gmail.com; ORCID: https://orcid.org/0000-0002-8536-4473.
[5]School of Applied Biosciences, Food & Agri-Tech, Rathinam Global Deemed to be University, Coimbatore, 641021, Tamil Nadu, India. Email: kamaraj.lordshiva@gmail.com.
*Correspondence: enishay30@gmail.com (N. M.); kamaraj.lordshiva@gmail.com (K. R.)

ABSTRACT
This study presents the fabrication and characterization of biocompatible starch/polyvinyl alcohol (PVA) electrospun nanoscaffolds incorporated with biogenic copper oxide (CuO) nanoparticles (NPs) synthesized using *Sargassum muticum* extract via an ultrasonic-assisted method. The synthesized CuO NPs exhibited a surface plasmon resonance (SPR) peak at 270 nm in UV-Vis spectroscopy, confirming nanoparticle formation. Fourier-transform infrared (FTIR) analysis revealed characteristic functional groups, including O–H stretching (3277 cm^{-1}) and Cu–O vibrations (600 cm^{-1}), validating successful NP integration into the scaffold. X-ray diffraction (XRD) confirmed the monoclinic crystalline phase of CuO NPs (JCPDS 05-0661), while Scanning electron microscopy (SEM) demonstrated a porous, fibrous scaffold structure with uniformly dispersed NPs. Thermogravimetric analysis (TGA) indicated thermal stability up to 243°C, with a residual mass of 51.88%. Dynamic light scattering (DLS) analysis showed an average NP size of 92.1 nm and a zeta potential of −12.62 mV, indicating moderate colloidal stability. Anti-inflammatory assays revealed that the starch/PVA/CuO-NP nanoscaffolds exhibited superior inhibition of protein denaturation (83.09% at 100 µg/mL) and xanthine oxidase activity (80.47% at 100 µg/mL) compared to free CuO NPs and algal extract, suggesting enhanced therapeutic efficacy due to synergistic effects. These findings highlight the potential of the developed nanoscaffolds as an advanced anti-inflammatory biomaterial for biomedical applications.

KEYWORDS: *Sargassum muticum*, Green synthesis, CuO NPs, Starch/PVA-nanoscaffolds, Anti-inflammatory activity.

1. INTRODUCTION

The rapid evolution of nanotechnology has catalyzed significant advancements in the development of functional nanomaterials for biomedical applications, particularly in drug delivery, tissue engineering, and anti-inflammatory therapies [1-6]. Among the wide spectrum of nanomaterials, metal oxide nanoparticles have garnered considerable interest due to their unique physicochemical properties, high surface area-to-volume ratio, and tunable biological functionalities [7-11]. Copper oxide nanoparticles (CuO NPs), in particular, have demonstrated potent antimicrobial, anticancer, antioxidant, and anti-inflammatory effects, making them ideal candidates for incorporation into advanced therapeutic platforms [12, 13]. However, the synthesis method employed significantly impacts their biocompatibility and functional performance [14]. Conventional chemical synthesis methods, while effective, often involve toxic reagents and harsh conditions that limit the biomedical applicability of the resulting nanoparticles [15]. In this context, green synthesis approaches have emerged as sustainable alternatives, utilizing biological extracts from plants, algae, or microorganisms to reduce metal precursors and stabilize nanoparticles under eco-friendly conditions [16].

Marine macroalgae, commonly known as seaweeds, are an underexplored but highly promising source of bioactive metabolites that can serve as reducing and capping agents in green nanomaterial synthesis [17]. Among

them, *Sargassum muticum*, a brown macroalgae species native to temperate coastal regions, has received increasing attention due to its rich biochemical profile [18]. This includes polysaccharides, phenolics, flavonoids, and sulfated compounds known for their antioxidant, anti-inflammatory, and metal-chelating capabilities [19]. These compounds not only facilitate the green synthesis of metal oxide nanoparticles but also confer added therapeutic value to the synthesized nanomaterials [20]. Moreover, employing ultrasonic-assisted extraction (UAE) techniques improves the yield and activity of bioactive molecules by enhancing cell wall disruption and mass transfer, thereby increasing the efficiency of the biosynthesis process [21-26].

The integration of green-synthesized CuO NPs into biocompatible scaffolds further enhances their utility in biomedical applications [27-31]. Nanofibrous scaffolds fabricated via electrospinning technology offer structural and functional advantages for therapeutic delivery and tissue regeneration [32, 33]. Electrospun nanofibers closely mimic the extracellular matrix (ECM) in terms of architecture and porosity, thereby supporting cell adhesion, proliferation, and differentiation [34]. Furthermore, the high surface area and interconnectivity of these fibers allow for effective loading and controlled release of therapeutic agents [35]. Among the various polymers employed for electrospinning, starch and polyvinyl alcohol (PVA) are particularly attractive due to their biocompatibility, biodegradability, and ease of processing [36]. Starch, a natural polysaccharide, provides structural stability and facilitates cell interactions, while PVA enhances mechanical strength and electrospinnability [37]. The combination of these polymers offers a versatile platform for incorporating nanoparticles without compromising scaffold integrity [38].

This study explored the fabrication of electrospun nanofibrous mats composed of starch/PVA blends loaded with CuO NPs synthesized using an ultrasonic-assisted green route employing *S. muticum* extract [39]. The biogenic synthesis strategy eliminates the use of hazardous chemicals and leverages the inherent therapeutic potential of marine-derived biomolecules [40]. The CuO NPs obtained through this route are expected to exhibit enhanced biocompatibility and therapeutic efficacy [41]. Furthermore, the incorporation of these nanoparticles into a polymeric matrix via electrospinning aims to produce a multifunctional scaffold capable of delivering anti-inflammatory effects in a controlled and sustained manner [42].

A comprehensive physicochemical characterization of the synthesized CuO NPs and the resulting electrospun nanofibrous scaffolds was undertaken to elucidate their morphology, functional groups, crystallinity, thermal stability, and surface properties [43]. UV-Vis spectroscopy confirmed nanoparticle formation through surface plasmon resonance characteristics [44]. Fourier-transform infrared (FTIR) analysis revealed the involvement of hydroxyl, phenolic, and carboxyl groups from the algal extract in nanoparticle stabilization [45]. X-ray diffraction (XRD) provided insights into the crystalline structure of CuO NPs and their incorporation within the fiber matrix [46]. Scanning electron microscopy (SEM) was employed to observe the fiber morphology, diameter uniformity, and nanoparticle distribution [47]. Thermogravimetric analysis (TGA) assessed the thermal stability and degradation behavior of the nanocomposite mats, which is critical for biomedical applications involving variable physiological conditions [48].

In addition to the physicochemical evaluation, the biological functionality of the nanofibrous scaffolds was assessed through anti-inflammatory activity assays [49]. Inflammation is a complex physiological response to injury or infection, but chronic or uncontrolled inflammation can lead to various pathologies including arthritis, cardiovascular diseases, and cancer [50]. Therefore, the development of materials with intrinsic anti-inflammatory properties holds considerable therapeutic promise [51]. The scaffolds and their components (CuO NPs and algal extract) were evaluated for their ability to inhibit protein denaturation and suppress xanthine oxidase activity—two widely used *in vitro* models to assess anti-inflammatory potential [52]. These assays provide critical insights into the biological compatibility and therapeutic relevance of the synthesized materials [53].

Overall, this research presents a sustainable and innovative approach for the development of multifunctional nanoscaffolds with enhanced physicochemical and biological properties [54]. By integrating marine algal biotechnology, green nanotechnology, and electrospinning, the study aims to advance the field of anti-inflammatory therapy and regenerative medicine [55]. The findings could pave the way for future investigations into marine-derived nanomaterials and their incorporation into advanced therapeutic systems such as wound healing dressings, implant coatings, and drug delivery devices [56]. Moreover, the use of *S. muticum*, a species often regarded as an invasive nuisance, adds an ecological dimension by promoting its valorization into value-added biomedical materials [57]. This aligns with broader global objectives related to sustainability, waste minimization, and marine resource utilization [58].

2. MATERIALS AND METHODS

2.1. Collection and preparation of marine macroalgae

Fresh *S. muticum* specimens were handpicked from the intertidal coastal zones near Rameswaram. The collected *Sargassum muticum* was taxonomically identified and authenticated by Dr V. Veeragurunathan, CSIR-CSMCRI-Marine Algal Research Station, Mandapam Camp 623519, Tamil Nadu, India. A voucher specimen was prepared and deposited at the Herbarium of the CSIR-CSMCRI-Marine Algal Research Station, under the accession number:

SI–2025–RMM–016. This authentication ensures botanical accuracy and standardization of the study material. The gathered samples were immediately placed in chilled containers to preserve their freshness during transportation to the laboratory. Upon arrival, the algal biomass was initially washed under running tap water to remove adhered sand particles, debris, and surface-dwelling organisms. This was followed by successive rinses using distilled water to ensure purity. The cleaned seaweed was then cut into smaller portions and left to air-dry in a shaded, well-ventilated room at ambient temperature for approximately two weeks. Once dried thoroughly, the samples were finely ground using a mechanical mill and the powdered material was stored in airtight containers at room temperature until further use.

2.2. Phytochemical extraction by ultrasonic treatment

For phytochemical extraction, 2 g of the dried and powdered *S. muticum* sample was mixed with 50 mL of Milli-Q water. The mixture underwent ultrasonic-assisted extraction using a LABQUEST ultrasonic cleaner (Borosil; Serial No. 941032329018) at 60°C for 45 minutes, enhancing the release of bioactive molecules through ultrasonic cavitation. Post-extraction, the mixture was filtered using Whatman No. 1 filter paper under sterile conditions to obtain a clear extract. The extract was stored at 10°C temporarily and then freeze-dried using a lyophilizer for long-term preservation and further use [59].

2.3. Green synthesis of CuO NPs

The synthesis process began by mixing 50 mL of 0.1 M $CuSO_4 \cdot 5H_2O$ solution with 10 mL of *S. muticum* extract (prepared by dissolving 10 mg of lyophilized powder in 10 mL Milli-Q water) in a 5:1 volume ratio. This mixture was stirred continuously at 650 rpm and heated to 60°C for two hours. A visual transformation in color from blue to bluish-green indicated the successful formation of CuO NPs via reduction of copper ions. The resultant mixture was centrifuged and washed three times with double-distilled water to eliminate residual organics and unreacted salts. The synthesized nanoparticles were freeze-dried for 48 hours and stored in a moisture-free environment for subsequent experiments and scaffold development [60].

2.4. Electrospinning of starch/PVA nanofibers containing CuO NPs

To produce nanocomposite mats, a 15% (w/w) PVA solution was prepared in Milli-Q water and stirred until fully dissolved. Subsequently, 100 mg each of starch and the synthesized CuO NPs were added. The solution was stirred rigorously at 50°C for 2.5 hours to ensure homogeneous dispersion. The final blend was then transferred into a syringe fitted with a stainless-steel needle (0.84 mm internal diameter) and mounted onto a HOLMARC HO-NFES-040 electrospinning setup. Optimized parameters included a voltage of 11.5 kV, a tip-to-collector distance of 12.3 cm, and a flow rate of 0.4 mL/h. Electrospinning was performed at room temperature for 6 to 8 hours. The resulting nanofiber mats were collected and stored in a desiccator until further characterization [61-63].

2.5. Physicochemical characterization of nanoparticles and electrospun mats

2.5.1. UV-Vis spectroscopic analysis

The optical characteristics of both *S. muticum* extract and synthesized CuO NPs were analyzed using a VIS SPEC V-730 spectrophotometer, scanning across a wavelength range of 200–800 nm. Deionized water was used as the blank. Characteristic surface plasmon resonance (SPR) peaks confirmed the formation of CuO NPs [64].

2.5.2. FTIR spectroscopy analysis

FTIR spectroscopy was carried out using a PerkinElmer Spectrum Two instrument in attenuated total reflectance (ATR) mode. Spectra were recorded between 4000 and 400 cm^{-1} at a resolution of 4 cm^{-1}, with 64 scans per sample. Functional group assignments focused on peaks related to hydroxyl, phenolic, carbonyl, and metal-oxygen linkages [65].

2.5.3. XRD analysis

Crystallographic features and phase purity of CuO NPs and composite nanofibers were assessed using a Bruker D8 Advance diffractometer with CuKα radiation (λ = 1.5406 Å), operating at 40 kV and 40 mA. Diffraction patterns were recorded in the 2θ range of 5° to 90°, using a step size of 0.029649°. The peaks were matched against JCPDS database standards for CuO confirmation [66].

2.5.4. SEM imaging analysis

Surface morphology and particle distribution were examined using a JEOL JSM-IT800 NANO SEM. Before imaging, samples were sputter-coated with a thin gold layer to improve conductivity. SEM micrographs were used to analyze fiber diameters, nanoparticle integration, and surface topology [67].

2.5.5. TGA

Thermal stability and decomposition profiles of the nanofiber composites were evaluated using a PerkinElmer TGA 8000 system. Around 5 mg of each sample was heated from room temperature to 550°C at a constant rate of 15°C/min under a nitrogen atmosphere. TGA plots provided data on moisture content, polymer degradation, and residual mass [68, 69].

2. 6. Particle size and zeta potential

The particle size distribution and surface charge of CuO NPs were assessed using a Malvern Zetasizer Ultra. Zeta potential values indicated colloidal stability, where high absolute values reflected strong electrostatic repulsion among particles [70].

All raw and processed data from the experiments are publicly available in the Mendeley Data repository, under the DOI: 10.17632/jrs2y2hp7v.2.

2.7. Anti-inflammatory activity assays

2.7.1. Inhibition of protein denaturation

Anti-inflammatory potential was tested using a modified heat-induced protein denaturation assay. Each reaction contained 0.45 mL of 5% bovine serum albumin solution and 0.05 mL of the test substance (*S. muticum* extract, CuO NPs, scaffold composite, or diclofenac sodium). Test concentrations used were 25, 50, 75, and 100 µg/mL. The pH was adjusted to 6.3 using 1 N HCl. Samples were incubated at 37°C for 20 minutes, followed by heating at 57°C for 3 minutes and cooling to room temperature. Absorbance was measured at 660 nm to assess protein denaturation [71].

2.7.2. Xanthine oxidase inhibition

The xanthine oxidase inhibitory effect was measured using a slightly modified standard method. Each assay included 0.3 mL of sample (*S. muticum* extract, CuO NPs, scaffolds, or diclofenac sodium) at different concentrations (25, 50, 75, 100 µg/mL), 0.5 mL of 0.15 mM xanthine (in phosphate buffer, pH 7.5), and 0.2 mL of xanthine oxidase (0.1 U/mL). After incubation for 15 minutes at 25°C, absorbance was recorded at 295 nm. A sample without enzyme served as the blank [72].

2.8. Statistical evaluation

Data from all experiments were analyzed using SPSS v25.0 and GraphPad Prism v9.0. Triplicate measurements were averaged and expressed as mean ± standard deviation. One-way ANOVA followed by Tukey's or Dunnett's post-hoc analysis was applied for statistical comparison ($p < 0.05$ considered significant). Data normality was assessed using the Shapiro–Wilk test. Where needed, data were log-transformed. Pearson's correlation coefficient was calculated to identify associations among variables. All statistical interpretations were based on a 95% confidence interval [73].

3. RESULTS

3.1. UV–Visible Spectroscopy

UV–Visible spectrophotometric evaluation (Fig. 1) of *S. muticum* extract and synthesized CuO NPs was conducted using a JASCO V-730 instrument across the 200–800 nm range at 1 nm intervals. The extract exhibited absorption features characteristic of natural phytochemicals, whereas the CuO NPs displayed a clear surface plasmon resonance (SPR) peak centered at 270 nm, confirming nanoparticle generation. The absorbance value recorded at 270 nm was 0.477617, validating effective synthesis. The spectrophotometer settings—1.0 nm slit width, 1000 nm/min scan rate, and automatic filter transitions—ensured precise data acquisition. This analysis illustrates the distinct optical behavior of the nanoparticles compared to the plant extract, with the SPR peak confirming their nanostructured identity [74].

3.2. FTIR spectroscopy analysis

FTIR analysis (Fig. 2) of CuO NPs and starch/PVA nanoscaffolds was performed using a PerkinElmer Spectrum Two instrument in ATR mode (4000–400 cm^{-1} range, 4 cm^{-1} resolution). For CuO NPs, broad O–H stretching bands appeared at 3277.29 cm^{-1}, while bands around 2700.50 cm^{-1} and 2500.00 cm^{-1} indicated C–H and possible carbonyl interactions. In contrast, the scaffold spectrum showed pronounced C=O stretching at 1500.00 cm^{-1} and a peak near 840.00 cm^{-1} corresponding to glycosidic linkages. Signals below 1000 cm^{-1}—particularly near 600.00 cm^{-1}—highlighted Cu–O vibrations, confirming the nanoparticles' integration. Overall, the spectral data affirm both structural consistency and the successful embedding of CuO NPs in the polymer matrix [75].

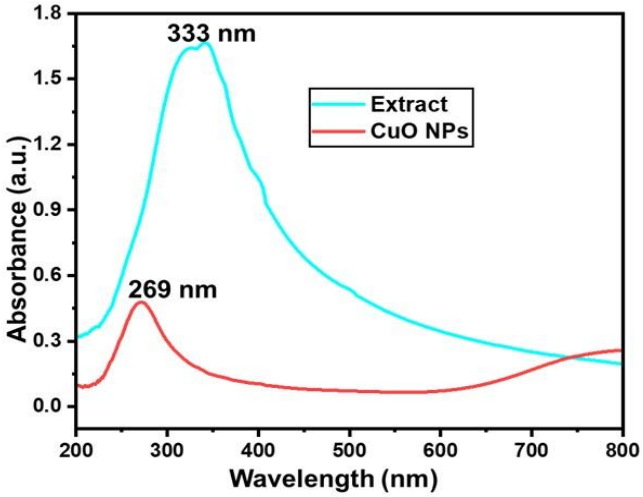

Fig. 1. UV–Visible spectral profiles of algal extract and CuO NPs.

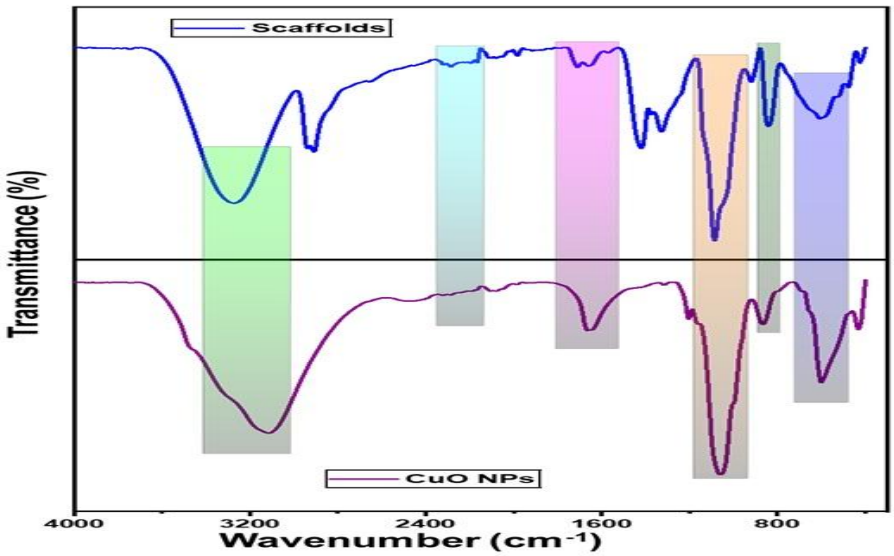

Fig. 2. FTIR spectra of CuO NPs and their incorporation into nanoscaffolds.

3.3. XRD analysis

XRD was carried out using a Bruker D8 Advance diffractometer with CuKα radiation, scanning from 5° to 90° 2θ. The CuO NPs exhibited diffraction peaks at 32.745° (110), 35.297° (002), 38.307° (111), and 48.123° (202), consistent with a monoclinic crystalline phase and matching JCPDS 05-0661. The starch/PVA scaffold displayed semicrystalline features with peaks at 19.270°, 21.364°, and 23.525°, while reflections at 26.536° and 29.481° (Fig. 3) suggested the influence of CuO NPs incorporation. Measured d-spacing values were 2.732 Å for CuO NPs and 4.602 Å for scaffolds. These findings confirmed the crystalline integrity of the CuO phase and its successful dispersion within the scaffold matrix [76].

3.4. SEM analysis

SEM using a JEOL JSM-IT800 NANO instrument revealed morphological differences between CuO NPs and starch/PVA nanoscaffolds (Fig. 4). The CuO NPs appeared as aggregated particles with spherical to irregular shapes. The nanoscaffold exhibited a porous and fibrous architecture. Uniform distribution of nanoparticles on the scaffold surfaces was observed, confirming effective integration. The scaffold's high porosity, coupled with a generally smooth texture and minor beading, demonstrates its potential for biomedical applications where high surface area and structural support are essential [77].

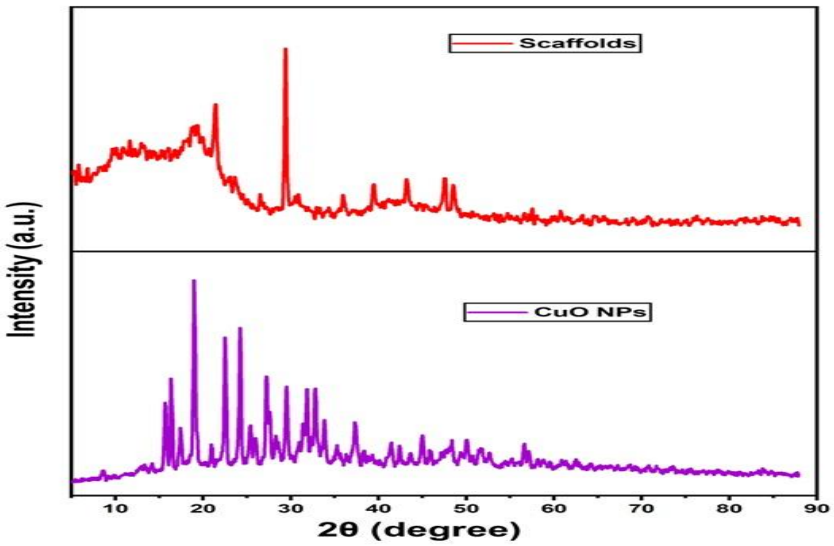

Fig. 3. XRD patterns of synthesized CuO NPs and CuO-loaded scaffolds.

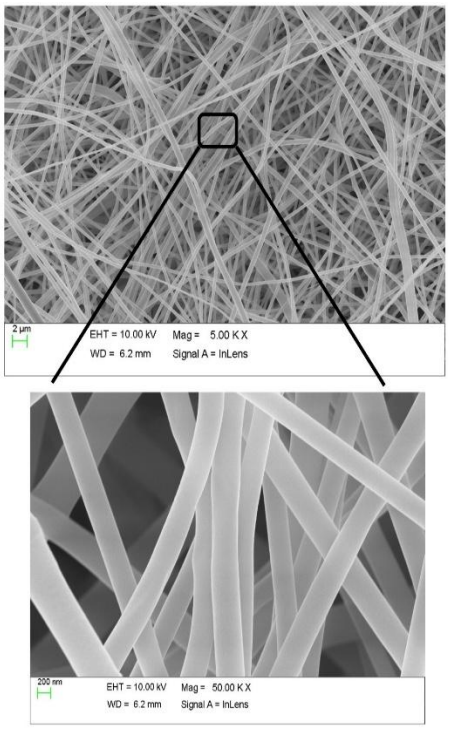

Fig. 4. SEM analysis of synthesized CuO NPs and CuO-loaded scaffolds.

3.5. TGA

Thermogravimetric profiling (Fig. 5) was performed using a PerkinElmer instrument under a nitrogen atmosphere over a temperature range of 25–550°C. The decomposition curve of the nanoscaffold revealed three major stages: initial moisture evaporation below 150°C, major polymer degradation initiating at 243.01°C and peaking at 349.62°C, and a final residual mass of 51.881%. The rapid mass reduction observed between 200°C and 400°C corresponded to starch and PVA decomposition. The relatively high remaining mass indicated the presence of crosslinked polymers or inorganic components, confirming thermal stability of the material up to 243°C [78].

3.6. Zeta potential and particle size analysis

Dynamic light scattering (DLS) using the Malvern Zetasizer Ultra determined the CuO NPs had an average hydrodynamic diameter (Z-average) of 92.1 nm (Fig. 6) with a polydispersity index (PDI) of 0.8444, indicating a moderately polydisperse size distribution. The measured zeta potential (Fig. 7) was −12.62 mV, with peak values at −20.85 mV and −8.994 mV, implying colloidal stability primarily governed by electrostatic repulsion. The system's conductivity was recorded at 0.07909 mS/cm, and the quality factor stood at 5.109, confirming the precision and reliability of the measurements. These parameters collectively reflect the nanoparticles' moderate colloidal stability within the suspension [79].

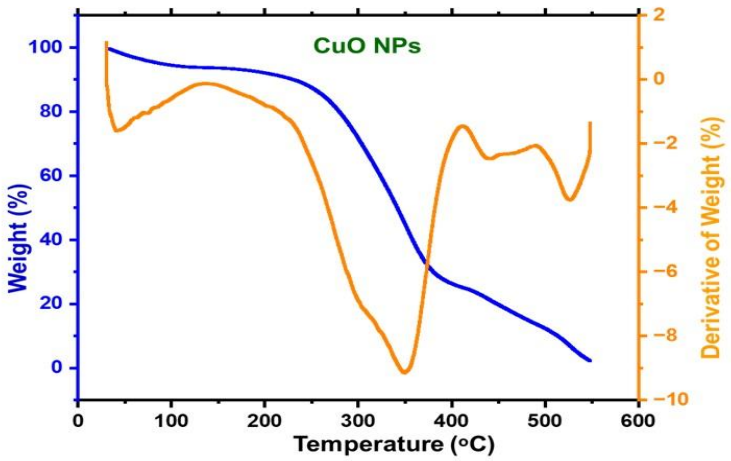

Fig. 5. Thermal degradation behavior of CuO-incorporated nanoscaffolds.

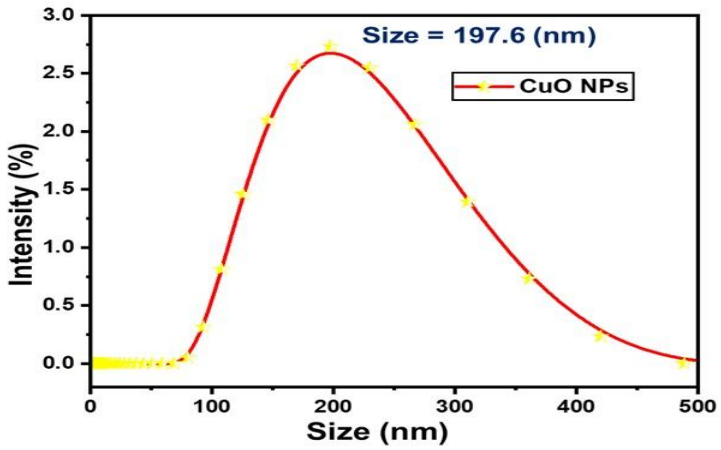

Fig.6. DLS particles size analysis of CuO NPs

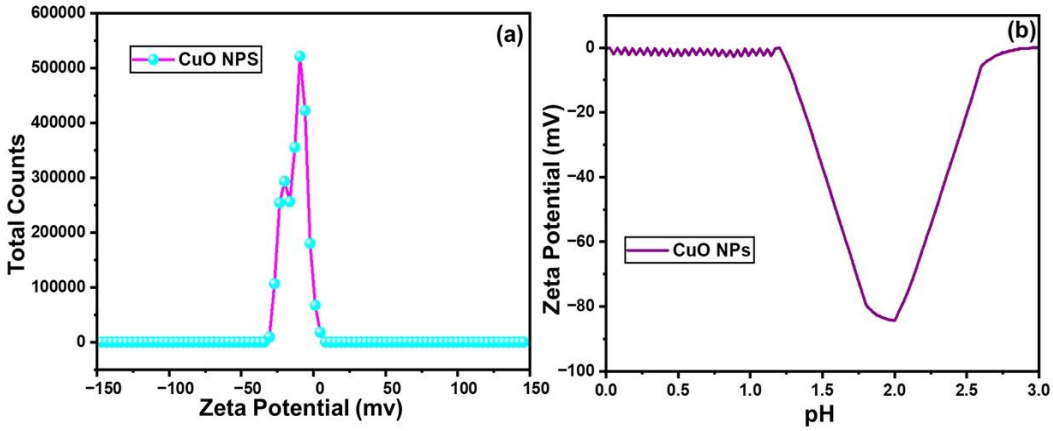

Fig.7. Zeta-potential analysis of CuO NPs

3.7. Anti-inflammatory assays

3.7.1. Protein denaturation inhibition assay

The protein denaturation inhibition assay (Fig. 8) evaluated the anti-inflammatory potential of algal extract, CuO NPs, and starch/PVA/CuO-NPs nanoscaffolds by measuring their ability to prevent heat-induced denaturation of bovine serum albumin (BSA). The results demonstrated concentration-dependent inhibition across all tested samples. At 25 µg/mL, the algal extract exhibited 22.88% inhibition, while CuO NPs and nanoscaffolds showed 26.88% and 29.88% inhibition, respectively. As the concentration increased to 50 µg/mL, the inhibition percentages rose to 38.29% (extract), 42.29% (CuO NPs), and 44.29% (nanoscaffolds). A further increase to 75 µg/mL resulted in 57.41% (extract), 62.41% (CuO NPs), and 66.41% (nanoscaffolds) inhibition. At the highest concentration (100 µg/mL), the extract displayed 67.09% inhibition, while CuO NPs and nanoscaffolds

exhibited 73.09% and 83.09%, respectively. Notably, the nanoscaffolds consistently outperformed both the algal extract and CuO NPs, suggesting enhanced anti-inflammatory activity, possibly due to the synergistic effects of the starch/PVA matrix and CuO NPs [80].

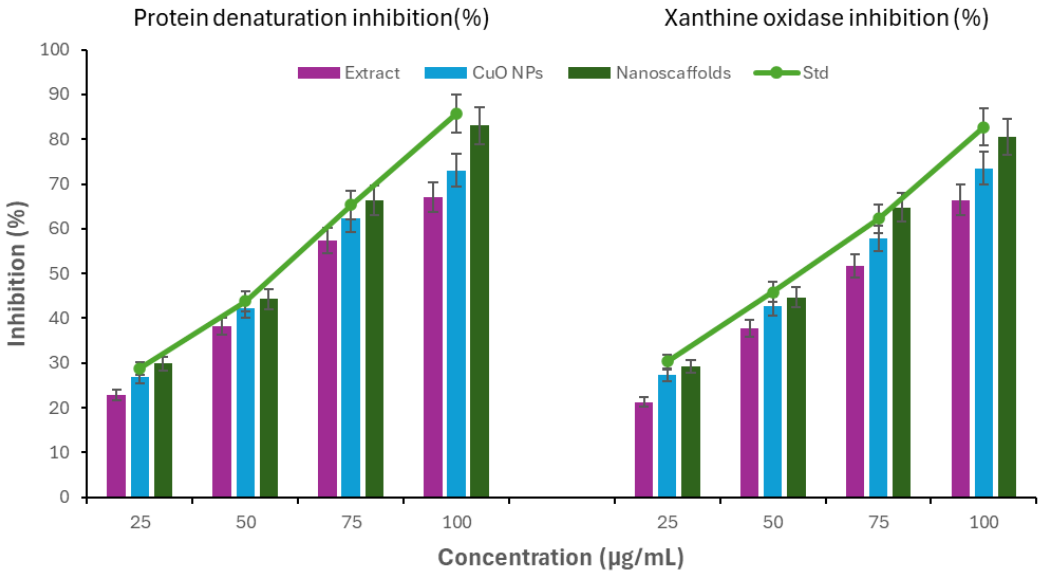

Fig.8. Anti-inflammatory activity analysis of algal extract, CuNPs and starch/PVA/CuONPs nanoscaffolds

3.7.2. Xanthine oxidase inhibition assay

The xanthine oxidase inhibition assay (Fig. 8) assessed the ability of the test samples to suppress uric acid production, a key factor in inflammation. Similar to the protein denaturation assay, concentration-dependent inhibition was observed. At 25 µg/mL, the algal extract inhibited xanthine oxidase by 21.27%, while CuO NPs and nanoscaffolds showed 27.27% and 29.27% inhibition, respectively. At 50 µg/mL, inhibition increased to 37.67% (extract), 42.67% (CuO NPs), and 44.67% (nanoscaffolds). Higher concentrations (75 µg/mL) led to 51.79% (extract), 57.79% (CuO NPs), and 64.79% (nanoscaffolds) inhibition. At 100 µg/mL, the extract exhibited 66.47% inhibition, while CuO NPs and nanoscaffolds demonstrated 73.47% and 80.47% inhibition, respectively. The nanoscaffolds again displayed superior inhibitory effects compared to the algal extract and CuO NPs alone, reinforcing their potential as an effective anti-inflammatory agent [81].

Both assays confirmed the anti-inflammatory properties of the tested samples, with starch/PVA/CuO-NPs nanoscaffolds exhibiting the highest efficacy. The results suggest that the nanoscaffolds could serve as a promising anti-inflammatory therapeutic, potentially due to enhanced stability and synergistic interactions between the components. Further studies could explore their mechanisms of action and *in vivo* applications.

4. DISCUSSION

The present study aimed to synthesize and characterize CuO NPs using *S. muticum* extract and incorporate them into starch/PVA nanoscaffolds for potential biomedical applications. A comprehensive analysis of the physicochemical properties and biological activity was carried out to evaluate their structural integrity, stability, and anti-inflammatory potential.

The UV–Visible spectroscopy analysis offered the first line of evidence for nanoparticle synthesis. The presence of a pronounced absorption peak at 270 nm for the CuO NPs, absent in the algal extract, confirmed the successful formation of CuO nanostructures. This peak is attributed to the surface plasmon resonance (SPR), a property characteristic of metal oxide nanoparticles. The SPR peak signifies the collective oscillation of conduction electrons induced by light, confirming the nanoscale dimensions of the synthesized particles. Furthermore, the sharpness and distinctiveness of the absorption band highlight the optical purity of the synthesized nanomaterials. The consistent baseline, appropriate scan parameters, and the use of 1.0 nm slit width and 1000 nm/min scan speed ensured accurate spectral acquisition [82].

FTIR spectroscopy further validated the synthesis by identifying functional groups involved in the reduction and stabilization processes. The CuO NPs spectrum displayed broad O–H stretching vibrations around 3277.29 cm^{-1}, possibly originating from phenolic groups in the algal extract, which likely played a role in the reduction of metal ions. Additional peaks near 2700.50 cm^{-1} and 2500.00 cm^{-1} indicated the presence of C–H and carbonyl groups. The starch/PVA scaffold, on the other hand, revealed characteristic glycosidic linkages and carbonyl (C=O) vibrations, confirming the polymer's structure. Notably, peaks below 1000 cm^{-1}, especially near 600.00 cm^{-1},

signified Cu–O stretching vibrations, confirming the integration of CuO NPs into the polymer matrix. These observations suggest successful conjugation without significant chemical disruption, which is critical for ensuring the structural functionality of the composite [83].

XRD analysis provided insight into the crystallinity of both the CuO NPs and the nanoscaffolds. The diffraction pattern of CuO NPs revealed distinct peaks matching standard JCPDS card 05-0661, verifying their monoclinic crystalline nature. This crystallinity is essential for stability and bioactivity. The scaffold exhibited a combination of amorphous and semicrystalline peaks attributed to starch and PVA. The appearance of additional peaks at 26.536° and 29.481° indicated the influence of CuO NPs on scaffold structure, possibly through partial alignment or reinforcement. Measured d-spacing values, 2.732 Å for CuO and 4.602 Å for the scaffold, supported this interpretation. These results suggest successful dispersion of crystalline CuO NPs within the biopolymer matrix, which may improve both mechanical and functional performance [84].

Morphological assessment via SEM revealed clear structural differences between the isolated CuO NPs and the fabricated scaffolds. The CuO particles appeared as aggregates with variable morphologies, including spherical and irregular forms. Such morphology is typical of green-synthesized metal oxide nanoparticles and can influence surface activity. The starch/PVA/CuO nanoscaffolds demonstrated a porous and fibrous texture with uniform distribution of nanoparticles across the scaffold surface. The high porosity observed is advantageous for biomedical applications, particularly in tissue engineering and drug delivery, as it facilitates nutrient transport and cellular infiltration. Minor beading observed on some fibers did not significantly compromise the uniformity, suggesting an optimized electrospinning process [85].

Thermogravimetric analysis highlighted the thermal behavior and stability of the nanocomposite. Three major degradation stages were observed: initial water loss, polymer breakdown, and residual stabilization. The major weight loss between 243.01°C and 349.62°C corresponded to the degradation of starch and PVA. The final residual mass of approximately 51.881% suggested the presence of thermally stable components such as inorganic CuO and possible crosslinked networks within the polymer. These findings affirm the scaffold's potential for use in thermally demanding biomedical environments [86].

Zeta potential and DLS analyses further confirmed the colloidal stability and size distribution of the CuO NPs. A Z-average particle size of 92.1 nm and a polydispersity index of 0.8444 indicated moderate polydispersity. Though not highly monodisperse, the size distribution remains within acceptable ranges for biomedical use. The zeta potential value of −12.62 mV suggested that electrostatic repulsion provides moderate colloidal stability. This is supported by peak values at −20.85 mV and −8.994 mV. The recorded conductivity (0.07909 mS/cm) and quality factor (5.109) confirmed the measurement's accuracy and reliability [87].

Biological evaluations, including protein denaturation and xanthine oxidase inhibition assays, provided strong evidence of anti-inflammatory activity. The CuO NPs and starch/PVA/CuO nanoscaffolds exhibited significant, dose-dependent inhibition of protein denaturation and xanthine oxidase activity. Notably, the nanoscaffold consistently outperformed both the algal extract and CuO NPs alone, reaching inhibition levels of 83.09% (protein denaturation) and 80.47% (xanthine oxidase) at 100 µg/mL. This enhanced activity is likely due to the synergistic effect of CuO's known anti-inflammatory properties and the biocompatibility of the starch/PVA matrix. The scaffold offers controlled release and structural support, contributing to sustained bioactivity [88].

The results confirm the successful synthesis of CuO NPs using *S. muticum* extract and their efficient incorporation into starch/PVA scaffolds. The nanocomposite demonstrates favorable physicochemical and biological properties, including thermal stability, appropriate morphology, moderate colloidal stability, and strong anti-inflammatory potential. These features highlight its promise for future applications in drug delivery, wound healing, and other therapeutic domains. Further *in vivo* studies are recommended to validate its clinical efficacy.

5. CONCLUSION

The present study successfully demonstrated the green synthesis of CuO NPs using *S. muticum* extract and their effective incorporation into starch/PVA nanoscaffolds. Characterization through UV–Vis spectroscopy, FTIR, XRD, SEM, TGA, and DLS analyses confirmed the formation, structural integration, thermal stability, and moderate colloidal stability of the CuO NPs and the developed scaffolds. Notably, the nanoscaffolds exhibited enhanced anti-inflammatory activity compared to both the algal extract and CuO NPs alone, as evidenced by protein denaturation and xanthine oxidase inhibition assays. The superior bioactivity is attributed to synergistic effects between the biopolymer matrix and embedded CuO NPs. These findings suggest that starch/PVA/CuO-NPs nanoscaffolds hold significant promise for biomedical applications, particularly in the development of anti-inflammatory therapies. Future investigations should focus on elucidating their precise mechanisms of action and evaluating their efficacy through comprehensive *in vivo* studies to advance their translational potential.

Funding: Not available for this study

Ethical Declaration: Not Applicable

Conflicts of Interest: The authors declare no conflicts of interest.

Data Availability Statement: The full dataset of physiochemical characterization associated with this work is published in Mendeley Data [Dataset] Bioactive nanostructured platforms: Physicochemical assessment of starch scaffolds hybridized with *Sargassum muticum*-copper oxide nanoparticles (DOI: 10.17632/jrs2y2hp7v.2). **Disclosure:** The material characterization data and figures (e.g., UV, SEM, FTIR, XRD, TGA, Zeta Potential and particle sizer) presented here were generated from a common dataset and are being reused across multiple related studies on nanomaterials. All biological analyses and conclusions are original to each manuscript.

REFERENCES

[1] Lavanya M, Krishnamoorthy R, Alshuniaber MA, Manoharadas S, Palanisamy CP, Veeraraghavan VP, Jayaraman S, Rajagopal P, Padmini R. Formulation, characterization and evaluation of gelatin-syringic acid/zinc oxide nanocomposite for its effective anticancer, antioxidant and anti-inflammatory activities. Journal of King Saud University-Science. 2023; 35: 102909.

[2] Palanisamy CP, Poompradub S, Sansanaphongpricha K, Jayaraman S, Subramani K, Sonsudin F. Biosynthesis of silver nanoparticles (AgNPs) using ethanolic extract of Nigella sativa (L.) seeds promotes wound healing via PDGF and VEGF signalling pathways activation. Biocatalysis and Agricultural Biotechnology. 2023; 54: 102970.

[3] Prasad M, Jayaraman S, Natarajan SR, Veeraraghavan VP, Krishnamoorthy R, Gatasheh MK, Palanisamy CP, Elrobh M. Piperine modulates IR/Akt/GLUT4 pathways to mitigate insulin resistance: Evidence from animal and computational studies. International Journal of Biological Macromolecules. 2023; 253: 127242.

[4] Palanisamy CP, Pei JJ, Phaniendra A, Venkata AAN, Jayaraman S, Veeraragahavan VP, Sridevi G, Roy JR, Janaki CS, Thalamati D, Mironescu M, Luo Q, Chai Y, Long Q. New Strategy of Neurodegenerative Disease Treatment with Extracellular Vesicles (EVs) Derived from Mesenchymal Stem Cells (MSCs). *Theranostics*. 2023; 13(12):4138-4165. doi:10.7150/thno.83066.

[5] Palanisamy CP, Phaniendra A, Jayaraman S, Poompradub S. *Nigella sativa* L. seed extracts promotes wound healing progress by activating VEGF and PDGF signalling pathways: *An in vitro* and *in silico* study. *F1000 Research*. 2023; 12: 436.

[6] Natarajan PM, Umapathy VR, Murali A, Swamikannu B. (2022). Computational Simulations of Identified marine-derived Natural Bioactive Compounds As Potential Inhibitors of Oral Cancer. Future Science OA. 2022; 8(3).

[7] Natarajan PM, Umapathy VR. Role of transcriptomics in the study of oral cancer. Frontiers in Oral Health. 2025; 6:1524364.

[8] Vidhyarekha U, Natarajan PM, Bhuminathan S, Sabarinathan J, Suba R, Vijayalakshmi P. Role of artificial intelligence in Oral Cancer. Advances in Public Health. 2024. 2024: 3664408.

[9] Ganesan A, Kumar NG, Natarajan PM, Gauthaman J. Automated classification of elongated styloid processes using deep learning models-an artificial intelligence diagnostics. Frontiers in Oral Health. 2025; 5: 1424840.

[10] Umapathy VR, Natarajan PM, Swamikannu B. Regenerative Strategies in Dentistry: Harnessing Stem Cells, Biomaterials and Bioactive Materials for Tissue Repair. Biomolecules. 2025; 15: 546.

[11] Natarajan PM. Dental Bioinformnatics-Current Scope and Future perspectives. Research Journal of Pharmacy and Technology. 2022;15(5):2351-6.

[12] Ganesan A, Kumar NG, Natarajan PM. Solanum trilobatum leaf extract-derived silver nanoparticles downregulate the PI3K/AKT/mTOR signaling pathway and attenuate oral squamous cell carcinoma cell proliferation. Journal of Herbmed Pharmacology. 2024; 13(2): 300-307.

[13] Perumal MKK, Renuka RR, Subbiah SK, Natarajan PM. Artificial intelligence-driven clinical decision support systems for early detection and precision therapy in oral cancer: a mini review. Frontiers in Oral Health. 2025; 6: 1592428.

[14] Ramesh E, Ganesan A, Lakshmi KC, Natarajan PM. Artificial intelligence-based diagnosis of oral leukoplakia using deep convolutional neural networks Xception and MobileNet-v2. Frontiers in Oral Health. 2025; 6: 1414524.

[15] Ganesan A, Kumar NG, Natarajan PM. Anticancer activity of silver nanoparticles synthesized from aqueous leaf extract of Solanum trilobatum (Purple fruit pea eggplant) on human oral cancer cells. Journal of Herbmed Pharmacololgy. 2024; 13(2): 260-268.

[16] Palanisamy CP, Poompradub S, Sansanaphongpricha K, Jayaraman S, Subramani K. Faridah Sonsudin gGreen synthesis of Nigella sativa-mediated silver nanoparticles for enhanced antibacterial activity and wound healing: Mechanistic insights and biomedical applications. Environmental Nanotechnology, Monitoring & Management. 2025; 24: 101085.

[17] Surendran N, Raju MV, Chandrasekaran MK, Ahalliya RM, Palanisamy CP, Chandrasekaran G, Kanniappan GV. Physicochemical characterization of starch from Maranta arundinacea L.(arrowroot)

rhizomes and its inhibition of COX-2: In vivo validation. Bioactive Carbohydrates and Dietary Fibre. 2025; 33: 100465.
[18] Kannappan P, Chandrasekaran MK, Raju MV, Gopalakrishnan S, Dhamodharan P, Ahalliya RM, Palanisamy CP, Raju B, Kanniappan GV. Exploring the anticancer potential of Jerantinine A from Tabernaemontana coronaria against prostate, breast, and ovarian cancers: a computational approach. Journal of Complementary and Integrative Medicine. 2025; 22(02): 363-372.
[19] Pei J, Kumarasamy RV, Jayaraman S, Kanniappan GV, Long Q, Palanisamy CP. Quercetin-functionalized nanomaterials: Innovative therapeutic avenues for Alzheimer's disease management. Ageing Research Reviews. 2025; 104: 102665.
[20] Jayaraman S, Prasad M, Natarajan SR, Krishnamoorthy R, Alshuniaber MA, Gatasheh MK, Veeraraghavan VP, Rajagopal P, Palanisamy CP. Molecular mechanisms underlying the effects of beta-sitosterol on TGF-β1/Nrf2/SIRT1/p53-mediated signaling in the kidney of a high-fat diet and sucrose-induced type-2 diabetic rat. Chemico-Biological Interactions. 2025; 411: 111443.
[21] Huang Y, Guo H, Liu Y, Jin W, Palanisamy CP, Pei J, Oz F, El-Aty AMA. Effects of Natural Polysaccharides on the Gut Microbiota Related to Human Metabolic Health. Molecular Nutrition & Food Research. 2025; e202400792.
[22] Prabhakaran P, Palanisamy CP, Shanmugam A, Damodharan P, Swaminathan H, Devaraj D, Ahalliya RM, Kanniappan GV. Isolation, structural characterization, and molecular docking studies on the bioactive compound from n-Hexane extract of Emilia sonchifolia (L.) DC against the pancreatic cancer target Aurora 2 Kinase. Journal of Complementary and Integrative Medicine. 2024; 22(1): 0290.
[23] Jiang H, Kumarasamy RV, Pei J, Raju K, Kanniappan GV, Palanisamy CP. Integrating engineered nanomaterials with extracellular vesicles: Advancing targeted drug delivery and biomedical applications. Frontiers in Nanotechnology. 2024; 6: 1513683.
[24] Guo H, Liu Y, Wan T, Song D, Palanisamy CP, Geng J, Pei J, Özmen S, El-Aty AMA. Toward personalized cancer management: Role of precision nutrition–diet interventions. Journal of Functional Foods. 2024; 123: 106584.
[25] Natarajan SR, Krishnamoorthy R, Alshuniaber MA, Al-Anazi KM, Farah MA, Rajagopal P, Palanisamy CP, Veeraraghavan VP, Jayaraman S. Identification of FOXM1 as a novel protein biomarker and therapeutic target for colorectal cancer progression: Evidence from immune infiltration and bioinformatic analyses. International Journal of Biological Macromolecules. 282 (Part 4): 137201.
[26] Rajendran MS, Jayaraman S, Khan JM, Jasmine S, Prabhakaran RK, Raju MV, Chandrasekaran MK, Ahalliya RM, Kannappan P, Palanisamy CP, Kanniappan GV. Investigating the colon toxicity and carcinogenic role of monosodium glutamate compared with Dimethylhydrazine in male Wistar rats: Exploring the link to childhood colon cancer risk. Journal of King Saud University - Science. 2024; 36(11): 103507.
[27] Kumarasamy RV, Natarajan P, Umapathy VR, Roy JR, Rab SO, Saeed M, Panagal M, Mironescu M, Srinivasan GP, Palanisamy CP. Clinical Applications and Therapeutic Potentials of Advanced Nanoparticles: A Comprehensive Review on Completed Human Clinical Trials. Frontiers in Nanotechnology. 2024; 6:1479993.
[28] Jin W, Pei JJ, Roy JR, Jayaraman S, Ahalliya RM, Kanniappan GV, Mironescu M, Palanisamy CP. Comprehensive review on single-cell RNA sequencing: A new frontier in Alzheimer's disease research. Ageing Research Reviews. 2024; 274: 102454.
[29] Pei J, Palanisamy CP, Jayaraman S, Natarajan PM, Umapathy VR, Roy JR, Panagal M, Jayaraman S. Curcumin-loaded polymeric nanomaterials as a novel therapeutic strategy for Alzheimer's disease: A comprehensive review. Ageing Research Reviews. 2024; 99: 102393.
[30] Pei J, Palanisamy CP, Jayaraman S, Natarajan PM, Umapathy VR, Roy JR, Thalamati D, Ahalliya RM, Kanniappan GV, Mironescu M. A comprehensive review on starch-based Sustainable Edible Films Loaded with Bioactive Components for Food Packaging. International Journal of Biological macromolecules. 2024; 274 (Part-1): 133332.
[31] Palanisamy CP, poompradub S, Sansanaphongpricha K, Subramani K, Sonsudin F. Increased expression levels of PDGF and VEGF magnify the wound healing potential facilitated by biogenic synthesis of silver nanoparticles. Nano-Structures & Nano-Objects. 2024; 39: 101236.
[32] Pei J, Palanisamy CP, Jayaraman S, Natarajan PM, Umapathy VR, Roy JR, Thalamati D, Ahalliya RM, Kanniappan GV, Mironescu M. Proteomics Profiling of Extracellular Vesicle for Identification of Potential Biomarkers in Alzheimer's Disease: A Comprehensive Review. Ageing Research Reviews. 2024; 99: 102359.
[33] Xi J, Wang T, Xian P, Liu X, Du M, Yang H, Palanisamy CP, Lin W, Long Q. Proteomic insights uncover enhanced neurotherapeutic potential in conditioned mesenchymal stem cell-derived extracellular vesicles. Extracellular Vesicle. 2024; 3: 100037.
[34] Pei J, Natarajan PM, Umapathy VR, Swamikannu B, Sivaraman NM, Krishnasamy L, Palanisamy CP. Advancements in the synthesis and functionalization of zinc oxide-based nanomaterials for enhanced oral cancer therapy. Molecules. 2024; 29(11): 2706.

[35] Gatasheh MK, Natarajan SR, Krishnamoorthy R, Alsulami TS, Rajagopal P, Palanisamy CP, Veeraraghavan VP, Jayaraman S. Molecular analysis to identify novel potential biomarkers as drug targets in colorectal cancer therapy: an integrated bioinformatics analysis. Molecular and Cellular Oncology. 2024; 11(1): 2326699.
[36] Pei J, Yan Y, Jayaraman S, Rajagopal P, Natarajan PM, Umapathy VR, Gopathy S, Roy JR, Sadagopan CS, Thalamati D, Palanisamy CP, Mironescu M. A review on advancements in the application of starch-based nanomaterials in biomedicine: Precision drug delivery and cancer therapy. International Journal of Biological Macromolecules. 2024; 130746.
[37] Pei JJ, Yan Y, Palanisamy CP, Jayaraman S, Natarajan PM, Umapathy VR, Gopathy S, Roy JR, Sadagopan JC, Thalamati D, Mironescu M. Materials-based drug delivery approaches: Recent advances and future perspectives. Green Processing and Synthesis. 2024; 13: 20230094.
[38] Pei JJ, Deng W, Liu Y, Guo Y, Chen J, Abdu H, Khan MR, Palanisamy CP, El-Aty AM. A Comprehensive Review of Cornus officinalis: Health Benefits, Phytochemistry, and Pharmacological Effects for Functional Drug and Food Development. Frontiers in Nutrition. 2023; 10: 1309963.
[39] Alugoju P, Palanisamy CP, Anthikapalli NVA, Jayaraman S, Prasanskulab A, Chuchawankul S, Dyavaiah M, Tencomnao T. Exploring the anti-aging potential of natural products and plant extracts in budding yeast Saccharomyces cerevisiae: A review. F1000Research. 2023; 12: 1265.
[40] Natarajan PM, Swamikannu B, Sivaraman NM, Stylin AGSQ. Prevention of Oral Cancer: A Comprehensive Guide. Journal of Pharmacy and Bioallied Sciences. 2024; 16(5): S4239-S4241.
[41] Umapathy V, Dhanavel A, Kesavan R, Natarajan PM, Bhuminathan S, Vijayalakshmi P. Anticancer Potential of the Principal Constituent of Piper nigrum, Piperine: A Comprehensive Review. Cureus. 2024; 16(2): e54425.
[42] Umapathy VR, Swamikannu B, Natarajan PM, Devi R, Nandini MS, Vimalarani, Vijayalakshmi P. In Silico Molecular Docking of Ocimum sanctum Phytochemicals: Targeting Key Biomarkers in Oral Cancer. Journal of Pharmacy and Bioallied Sciences. 2024; 16(5): S4792-S4799.
[43] Natarajan PM, Bhuminathan S, Rajan R, Bindu K, Loganathan K, Veerakumar R. The Crucial Role of Smoking Cessation in Preventing Oral Cancer. Journal of Pharmacy and Bioallied Sciences. 2024; 16(5): S4245-S4247.
[44] Swamikannu B, Umapathy VR, Natarajan PM, Nandini MS, Stylin AGSQ, Vimalarani V, Rajinikanth S. Unlocking the Therapeutic Benefits of Artemisia Annua: A Comprehensive Overview of its Medicinal Properties. Journal of Pharmacy and Bioallied Sciences. 2024; 16(5): S4248-S4253.
[45] Natarajan PM. Computational Studies on Recent Congeners of Fluoroquinolones and Nitroimidazoles for Their Use in Periodontal Therapy. Journal of Pharmacy and Bioallied Sciences. 2024; 16(5): S4731-S4740.
[46] Yadalam PK, Arumuganainar D, Natarajan PM, Ardila CM. Artificial intelligence-powered prediction of AIM-2 inflammasome sequences using transformers and graph attention networks in periodontal inflammation. Scientific Reports. 2025; 15: 8733.
[47] Yadalam PK, Chatterjee S, Natarajan PM, Ardila CM. Comparison of light gradient boosting and logistic regression for interactomic hub genes in Porphyromonas gingivalis and Fusobacterium nucleatum-induc ed periodontitis with Alzheimer's disease. Frontiers in Oral Health. 2025; 6:1463458.
[48] Natarajan PM, Bhuminathan S, Leela B, Bindu K, Loganathan K, Ramachandran V. Smoking and its Role in Oral Cancer. Journal of Pharmacy and Bioallied Sciences 16(5): S4242-S4244.
[49] Yadalam PK, Natarajan PM, Ardila CM. Variational graph autoencoder for reconstructed transcriptomic data associated with NLRP3 mediated pyroptosis in periodontitis. Scientific Reports. 2025; 15: 1962.
[50] Kunamalla RP, Panagal M, Palanisamy CP. Green-engineered multiscale starch/PVA nanofibrous scaffolds embedded with CuO nanoparticles from *Sargassum ilicifolium* for potent antimicrobial performance. Genetics and Molecular Research. 2026; 25 (13s): 1-8.
[51] Daniel Raja FS, Abraham L, Rangasamy K, Saikia K, Rathankumar AK, Mironescu M, Mironescu I, Palanisamy CP, Kanniappan GV. Next-Generation Microbiome Therapeutics: Psychobiotics and Fecal Microbiota Transplants (FMT) for Mental Health Treatment. Frontiers in Cellular and Infection Microbiology. 2026; 16: 1719357.
[52] Dharmaprakash S, Gunasekaran VP, Sivaramakrishnan R, Kanniappan GV, Jayaraman S, Mironescu M, Rajabathar JR, Mironescu ID, Palanisamy CP. Marine macroalgae-mediated ultrasonic-assisted green synthesis of CuO nanoparticles embedded in starch/PVA electrospun nanoscaffolds for in vitro α-amylase and α-glucosidase inhibitory activity. Scientific Reports. 2026.
[53] Surendran N, Chandrasekaran G, Raju MV, Chandrasekaran MK, Ahalliya RM, Palanisamy CP, Kanniappan GV, Arcot R, Alharbi NS, Thiruvengadam M. Anti-inflammatory potential of ethanolic extract of Maranta arundinacea L.: Insights from COX-2 modulation and oxidative stress analysis. South African Journal of Botany. 2026; 195: 142-151.
[54] Pei J, Senthilkumar MV, Hessini K, Subramaniyam S, Sivaramakrishnan R, Kanniappan GV, Jayaraman S, Palanisamy CP. Green fabrication of starch/PVA/CuO nanoscaffolds using marine macroalgae extract for enhanced anti-inflammatory activity. Sustainable Chemistry and Pharmacy. 2026; 51: 102397.
[55] Balasubramanian V, Loganathan L, Muthuswamy K, Viswanathan TM, Raju MV, Chandrasekaran MK, Ahalliya RM, Poorasamy J, Palanisamy CP, Dominic S, Kanniappan GV. Anticancer therapeutic efficacy

of PEGylated β-galactosidase from Aspergillus terreus in DMBA-induced breast cancer: Toxicological, molecular and histopathological evaluation in Wistar rats. International Journal of Biological Macromolecules. 2026; 360: 151856.
[56] Jayaraman S, Eswaran A, Rajagopal P, Palanisamy CP, Veerakumar P, Veeraraghavan VP, Sirasanagandla SR. Neuroendocrine-associated epigenetic factors in cellular senescence: mechanisms and therapeutic implications. Biogerontology. 2026; 27(2): 64.
[57] Ponnusamy B, Rajagopal P, Palanisamy CP, Veeraraghavan VP, Jayaraman S. Mechanistic Exploration of the anticancer activity of Justicia adhatoda Plant Leaf Ethanolic Extract against Colon Cancer Cells: An in silico and in vitro Approach. Asian Pacific Journal of Cancer Prevention. 2026; 27(3): 1069-1080.
[58] Pei J, Saran VS, Sivaramakrishnan R, Kanniappan GV, Pandurangan V, Jayaraman S, Dhayalan VK, Mironescu M, Mironescu ID, Palanisamy CP. Ultrasonic-assisted, Sargassum ilicifolium (brown marine macroalgae)-mediated biogenic synthesis of CuO nanoparticles incorporated in starch/PVA electrospun nanoscaffolds: In vitro safety and antioxidant efficacy assessment. Bioorganic Chemistry. 2026; 173: 109679.
[59] Raj MAPA, Subramaniyam S, Kanniappan GV, Jayaraman S, Palanisamy CP. Sustainable fabrication of starch/PVA/CuO electrospun nanoscaffolds from Turbinaria ornata (marine macroalgae) extract: Physicochemical characterization and antidiabetic evaluation. Kuwait Journal of Science. 2026; 53(2): 100545.
[60] Pei J, Ganesh NS, Subramaniyam S, Sivaramakrishnan R, Kanniappan GV, Jayaraman S, Palanisamy CP. Sustainable fabrication of starch/PVA/CuO electrospun nanoscaffolds from Padina tetrastromatica (Brown macroalgae) extract: Physicochemical characterization and antidiabetic assessment. Sustainable Chemistry One World. 2026; 9: 100195.
[61] Sakthiraj A, Sivaramakrishnan R, Subramaniyam S, Kanniappan GV, Pandurangan V, Jayaraman S, Dhayalan VK, Mironescu M, Mironescu ID, Palanisamy CP. Starch/PVA electrospun nanoscaffolds loaded with ultrasonic-assisted green-synthesis of CuO nanoparticles from marine macroalgae (Gracilaria corticata) extract: Cytotoxicity and antioxidant analysis. Chemical Physics Impact. 2026; 12: 101018.
[62] Raju M, Chandrasekaran MK, Loganathan L, Ahalliya RM, Mironescu M, Mironescu ID, Palanisamy CP, Kanniappan GV. Lipid remodeling and ferroptosis in phosphatidylcholine-mediated tumor–stroma crosstalk. Frontiers in Molecular Biosciences. 2026; 13: 1742305.
[63] Kunamalla R, Panagal M, Palanisamy CP. Biogenic synthesis and fabrication of starch/PVA/CuO electrospun nanoscaffolds from Sargassum ilicifolium (brown marine macroalgae) extract for anticancer activity on HT-29 and MCF-7 cancer cells. Biocatalysis and Agricultural Biotechnology. 2026; 72: 103923.
[64] Pei J, Govindaraj H, Sivaramakrishnan R, Kanniappan GV, Pandurangan V, Dhayalan VK, Mironescu M, Mironescu ID, Jayaraman S, Palanisamy PC. Sustainable fabrication of biopolymer-based (starch/PVA) nanoscaffolds loaded with green-synthesized CuO nanoparticles from Sargassum wightii (marine macroalgae): Cytocompatibility and antioxidant activity. Biomaterials Advances. 2026; 182: 214660.
[65] Pei J, Perumal NC, Meng P, Long Q, Palanisamy CP. Extracellular vesicle-based biosensors for Alzheimer's disease: A new frontier in precision diagnostics. Ageing Research Reviews. 2026; 113: 102904.
[66] Shree P, Sivaramakrishnan R, Kanniappan GV, Pandurangan V, Jayaraman S, Dhayalan VK, Mironescu M, Mironescu ID, Palanisamy CP. Antioxidant and biocompatible CuO-starch/PVA nanoscaffolds via ultrasonic green synthesis using Turbinaria conoides (brown marine macroalgae). Medicine in Drug Discovery. 2025; 28: 100238.
[67] Gong J, Lin J, Guan T, Pei J, Palanisamy CP, El-AtyFrom AMA. selenium tolerance to nanoplastic antagonism: Comprehensive characterization of L. casei SNUT1 and its extracellular vesicle–nanoselenium complex. Food Bioscience. 2025; 74: 107749.
[68] Poochi SP, Sundarraj R, Raju MV, Chandrasekaran MK, Ahalliya RM, Palanisamy CP, Kanniappan GV, Kondapavuluri BK, Thiruvengadam M. Harnessing Nature: Computational and Experimental Insights Into *Ipomoea obscura* Metabolites for Bladder Cancer Therapy. Chemistry and Biodiversity. 2025; 0: e00909.
[69] Dugganaboyana GK, Kannankumar MKG, Shivaramakrishna S, Raju MV, Chandrasekaran MK, Ahalliya RM, Panneerselvam N, Palanisamy CP, Kanniappan GV. Phytochemical insights, antioxidant activity and therapeutic potential of Cassia senna against prostate cancer in Wistar albino rats. Discover Applied Sciences. 2025; 7:1206.
[70] Natarajan SR, Krishnamoorthy R, Alshuniaber MA, Gatasheh MK, Rajagopal P, Veeraraghavan VP, Palanisamy CP, Jayaraman S. KDM1A Facilitates Oncogenic Potential in Colorectal Cancer Progression Through the Activation of AXIN/GSK3β/β-Catenin Signaling Pathways: Evidence From Integrated Transcriptomics and In Vitro Studies. The Journal of Gene Medicine. 2025; 27(11): e70053.
[71] Guan T, Gong J, Lin J, Palanisamy CP, Jinjin Pei J, El-Aty AMA. Machine learning-driven multimodal optimization of selenium biotransformation and flavor profiling in fermented apple–Yacon functional beverages. Innovative Food Science & Emerging Technologies. 2025; 105: 104198.
[72] Natarajan SR, Krishnamoorthy R, Alshuniaber MA, Alsulami TS, Gatasheh MK, Rajagopal P, Palanisamy CP, Govindan R, Veeraraghavan VP, Jayaraman S. ABCE1 facilitates tumour progression via aerobic glycolysis and inhibits cell death in human colorectal cancer cells through the p53 signalling

pathway. Scientific Reports. 2025; 15: 24674.
[73] Huang Y, Guo H, Liu Y, Jin W, Palanisamy CP, Pei J, Oz F, El-Aty AMA. Effects of Natural Polysaccharides on the Gut Microbiota Related to Human Metabolic Health. Molecular Nutrition & Food Research. 2025; 69:e202400792.
[74] Poornima K, Meenakshi K.C, Manikandan V.R, Shankari G, Prabhu D, Rathi M.A, Palanisamy CP, Balaji R, Gopalakrishnan V.K. Exploring the anticancer potential of Jerantinine A from *Tabernaemontana coronaria* against prostate, breast, and ovarian cancers: A computational approach. *Journal of Complementary and Integrative Medicine*, 2025 22(2): 363–372.
[75] Manimaran D, Elangovan N, Mani P, Subramanian K, Ali D, Alarifi S, Palanisamy CP, Zhang H, Rangasamy K, Palanisamy V, Mani R, Govarthanan K, Aruni W, Shanmugam R, Srinivasan GP, Kalirajan A. Isolongifolene-loaded chitosan nanoparticles synthesis and characterization for cancer treatment. Scientific Reports. 2022; 12:19250.
[76] Palanisamy CP, Cui B, Zhang H, Gunasekaran VP, Ariyo A, Jayaraman S, Veeraraghavan V, Rajagopal P. A critical review on starch-based electrospun nanofibrous scaffolds for wound healing application. International Journal of Biological Macromolecules. 2022; 222 (Part: B): 1852-1860.
[77] Pei J, Umapathy VR, Vengadassalapathy S, Hussain SFJ, Rajagopal P, Jayaraman S, Veeraraghavan VP, Palanisamy CP, Gopinath K. A Review of the Potential Conse-quences of Pearl Millet (Pennisetum glaucum) for Diabetes Mellitus and Other Biomedical Applications. Nutrients. 2022; 14(14):2932.
[78] Monisha P, Ponnulakshmi R, Nalini D, Vishnu P V, Palanisamy CP, Cui B, Shankargouda P, Selvaraj J. A comprehensive review on high fat diet-induced diabetes mellitus: An epigenetic view. The Journal of Nutritional Biochemistry. 2022; 2022: 109037.
[79] Monisha P, Selvaraj J, Mohamed AE, Mohamed E, Mosaab AEA, Vishnu PV, Srinivasan V, Vidhya RU, Shazia FJH, Kalaiselvi K, Durairaj S, Palanisamy CP, Surapaneni K M, Ponnulakshmi R. A Comprehensive review on therapeutic perspectives of phytosterols in insulin resistance: A mechanistic approach. Molecules. 2022; 27(5): 1595.
[80] Kannayiram K, Umapathy VR, Chamundeswari Y, Fathima JH, Govindan R, Palanisamy CP, Veeraraghavan VP, Jayaraman S, Rajagopal P. Molecular docking analysis of flavonoids with aldose reductase. Bioinformation. 2022; 18(3): 80–83.
[81] UV Rekha, Varadhachariyar R, Rajagopal P, Priya PH, Fathima JHS, Govindan R, Palanisamy CP, Veeraraghavan VP, Jayaraman S. Molecular docking analysis of bioactive compounds from Plectranthus amboinicus with glucokinase. Bioinformation. 2022; 18(3): 261–264.
[82] Umapathy VR, Rajagopal P, Varadhachariyar R, Priya PH, Fathima JHS, Govindan R, Palanisamy CP, Brindha KBA, Veeraraghavan VP, Jayaraman S. Molecular docking analysis of bioactive compounds from Cissampelos pareira with PPAR gamma. Bioinformation. 2022; 18(3): 265-268.
[83] Rajagopal P, Umapathy VR, Sandhya P, Fathima JH, Govindan R, Palanisamy CP, Veeraraghavan VP, Jayaraman S. Molecular docking analysis of metformin analogues with GSK-3β. Bioinformation. 2022; 18(3): 269-272.
[84] Adeniran LA, Palanisamy CP, Ashafa AOT. Chemical profiling, in vitro antioxidant and antidiabetic assessment of flavonoids from the ethanol extract of Hermannia geniculata root. Sokoto Journal of Veterinary Sciences. 2021; 19(1): 1-13.
[85] Sundaram S, Palanisamy CP, Subban R, Palanirajan A, Piramanayagam S, Eswaran M, Krishna CK, Kanniappan VG. 1-Pentacosanol Isolated from Stem Ethanolic Extract of Cayratia trifolia (L.) is A Potential Target for Prostate Cancer-In SILICO Approach. Jordan Journal of Biological Sciences. 2021; 14 (2): 359-365.
[86] Raj SS, Palanisamy CP, Mani P. Antioxidant, antimicrobial and cytotoxicity of n-hexane extract from Mollugo nudicaulis Lam. Bioinformation. 2021; 17 (5), 573-582.
[87] Palanisamy CP, Cui B, Zhang H, Panagal M, Paramasivam S, Chinnaiyan U, Jeyaraman S, Murugesan K, Rostagno M, Sekar V, Natarajan SP. Anti-ovarian cancer potential of phytocompound and extract from South African medicinal plants and their role in the development of chemotherapeutic agents. American Journal of Cancer Research. 2021; 11(5):1828-1844.
[88] Jayaraman S, Devarajan N, Rajagopal P, Babu S, Ganesan SK, Veeraraghavan VP, Palanisamy CP, Cui B, Periyasamy V, Chandrasekar K. β-Sitosterol Circumvents Obesity Induced Inflammation and Insulin Resistance by down-Regulating IKKβ/NF-κB and JNK Signaling Pathway in Adipocytes of Type 2 Diabetic Rats. Molecules. 2021; 26: 2101.